

Novel *A15* phase in barium-doped fullerite

A. R. Kortan, N. Kopylov, R. M. Fleming, O. Zhou, F. A. Thiel, and R. C. Haddon
AT&T Bell Laboratories, Murray Hill, New Jersey 07974

K. M. Rabe

Department of Applied Physics, Yale University, New Haven, Connecticut 06520

(Received 20 November 1992)

A new stable compound Ba_3C_{60} is reported in the Ba-C_{60} phase diagram. Rietveld refinement of x-ray powder diffraction data shows that this compound has the *A15* structure with a lattice constant of 11.34 Å. The $Pm\bar{3}n$ space group implies a perfect alternating orientational order for the C_{60} molecules, not previously observed in doped fullerite structures. The relative stability of the *A15* phase over the fully intercalated fcc structure can be explained by a simple model involving the Madelung energy differences, orientation dependence of the C_{60} -cation interaction energy, and distortion-induced relaxational energy gains.

Interest in doped fullerite systems, stimulated by superconductivity in $(\text{K,Rb,Cs})_3\text{C}_{60}$,¹⁻⁴ Ca_5C_{60} ,⁵ and Ba_6C_{60} ,⁶ as well as their other structural and electronic properties,⁷⁻⁹ has prompted intensive exploration of the phase diagrams of C_{60} with alkali metals, alkaline earths, and other elements. In this paper, we report the synthesis and structure determination of the compound Ba_3C_{60} . The new features observed in this compound illuminate basic principles underlying the structure and properties of doped fullerites. First, Ba_3C_{60} has the *A15* structure rather than the fully intercalated fcc structure¹⁰ of the alkali-metal fullerites $(\text{K,Rb,Cs})_3\text{C}_{60}$. We will show that a very simple model of the structural energetics of doped fullerites is sufficient for a basic understanding of this and of other chemical trends in crystal structure. In fact, the energetically competitive nature of the *A15* structure at $x=3$ was first predicted theoretically within such an approach.^{11,12} With the structural data reported here we will be able to discuss in more detail the factors favoring the *A15* phase in this system. In addition, the Ba_3C_{60} structure shows a type of molecular orientational order, not previously observed in doped fullerite compounds, in which molecules and their neighbors alternate between two orientations related by a 90° rotation. This suggests that identification of the type of molecular orientational order should be regarded as an essential aspect of structural characterization.

Samples are prepared from chromatographically purified and vacuum outgassed C_{60} . High-purity barium metal is broken into a powder and mixed with C_{60} in a controlled atmosphere glove box. Powder mixtures are pressed into pellets in custom-designed high-purity tantalum cells and, loaded into quartz tubes without removing them from the tantalum cells. Other samples were prepared by loading the quartz tubes with unpressed powder mixtures. Quartz tubes are then sealed under a vacuum of 10^{-6} Torr. Heat treatments were carried out at temperatures 550–800°C, and for periods ranging from hours to weeks. Slow diffusion of barium in C_{60} creates serious problems with sample uniformity at temperatures lower than 600°C. Highly uniform samples are

prepared by few-day anneals at higher temperatures. Powders are then removed from the tantalum cells loaded into quartz x-ray capillaries, and again sealed under high vacuum.

Powder x-ray diffraction measurements were carried out with Mo $K\alpha$ radiation on a 12-kW rotating anode generator equipped with a triple axis goniometer. Flat ZYA graphite crystals were used to monochromatize and analyze the x-ray beam with a longitudinal resolution of 10^{-2} Å⁻¹. Samples are rocked 6° at each two-theta data point to obtain a statistically averaged powder pattern.

Samples prepared with barium concentration in the vicinity of $x=3$ exhibited a powder x-ray diffraction pattern that could not be fitted to any of the known fullerite phases. The unit cell of this phase is identified as a primitive cubic cell with a lattice parameter of 11.34 Å. This lattice parameter being close to a bcc fullerite cell parameter, we next attempted to refine the diffraction data to establish the arrangement of the cations, assuming a bcc packing of the C_{60} molecules. The number of interstitial sites increases from three per C_{60} in an fcc sphere packing to six in a bcc sphere packing. Additionally, the distinction between octahedral and tetrahedral sites is removed in the bcc sphere packing, all interstitial sites becoming equivalent with distorted tetrahedral symmetry. These sites are 31% larger than the tetrahedral sites of the fcc sphere packing. Out of all the possible $x=3$ structures based on a bcc C_{60} packing with cations in the tetrahedral holes, the *A15* phase is the only one with cubic symmetry. This structure, with barium atoms forming three nonintersecting orthogonal chains along the cube faces, as shown in Fig. 1, is familiar from the Nb_3Sn family of compound superconductors.¹³

The x-ray powder intensities were analyzed using the GSAS Rietveld refinement package. Figure 2 shows fitted data to a model of the *A15* structure [space group $Pm\bar{3}n$; Fig. 1(a)] with parameters as shown in Table I. A C_{60} molecule with equal bond lengths was used. Carbon positions were only allowed to vary radially to preserve the shape of the C_{60} molecule. The $Pm\bar{3}n$ space group orders the centers of the C_{60} molecules on a bcc sublattice

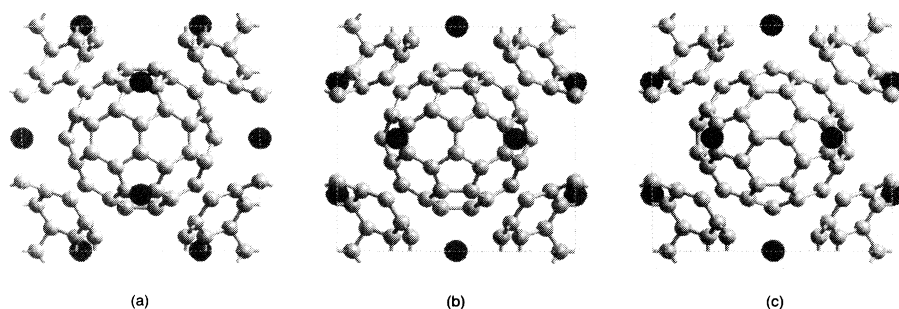


FIG. 1. Structural models of the Ba_3C_{60} $A15$ phase. Barium cations occupying the interstitial sites defined by five-membered rings (a), and six-membered rings (b) of the neighboring molecules. Orientationally aligned molecules define the $Pm\bar{3}$ structure in (c).

with the twofold axis of the body-center molecule rotated by 90° with respect to the molecule at the origin. (The twofold axis is a line through the molecule center and the center of the double bond.) This is in contrast to the alkali-doped bcc structures of C_{60} (space group $Im\bar{3}$). In A_6C_{60} , $A = K, Rb, Cs$, the center molecule differs from the molecule at the origin only by a translation. This results in the $A15$ structure having two types of sites for Ba doping, one that faces only five-membered rings [Fig. 1(a)] on the surface of the C_{60} neighbors and one that faces only six-membered rings [Fig. 1(b)]. For the C_{60} orientation we have chosen in Table I, site $6c$ faces five-membered rings and site $6d$ faces six-membered rings. We find that in the Rietveld refinement, site $6c$, the “five-membered ring” site is preferred over the $6d$ site with integrated R factors of $R_i = 11.9\%$ and 13.2% , respectively. Using the Hamilton¹⁴ test, the probability that Ba is located in $6d$ instead of $6c$ is less than 1%. Ordering the C_{60} sublattice with parallel double-bond directions as in A_6C_{60} requires a lowering of symmetry to $Pm\bar{3}$. We find little change in the R factor if we lower the symmetry to $Pm\bar{3}$ and use the same positions given in Table I. We observe about a 1% increase in the R factor of the $Pm\bar{3}$ refinement if the center molecule is rotated to give parallel double-bond directions. The intensity of the 230 peak was particularly sensitive to the details of the models shown in Fig. 1. Rietveld refinements (Fig. 2 inset) favored model (a) as the best candidate. This suggests that ordered, 90° rotation of the center C_{60} molecule is a real effect with Ba atoms located above five-membered

rings. Five-membered rings of the molecules are believed to be electron deficient; therefore, these sites may be energetically very favorable for divalent cations as will be discussed below. In alkali-metal-doped fcc structures, both tetrahedral and octahedral cation interstitial sites are surrounded by six-membered rings of the neighboring molecules¹⁰ alone. The increased charge transfer in the divalent systems preferring five-membered rings nearby may explain the stability of the $A15$ phase for the divalent cations case.

As in fcc $x = 3$ structure, the presence of some kind of molecular orientational order is required by constraints on cation-C distances. In the fcc case, this limits the possibilities to two (eight of the 20 hexagonal faces aligned along 111) related by 90° rotation. In the observed structure, the two orientations occur randomly, with equal probability.¹⁰ All the tetrahedral holes are surrounded by four hexagons of the four surrounding molecules and the C-K distance is 3.27 Å. In the $x = 6$ bcc packing, all balls are equivalent and orientationally uniform, and all the tetrahedral holes are equivalent and surrounded by two pentagons and two hexagons. In the $A15$ structure, the different orientational order of the molecules yields two different tetrahedral sites, with one facing four hexagons from the surrounding balls and the other four pentagons. As described above, we find that all the pentagon holes are occupied and all the hexagon holes are empty.

With these orientations, we can compute the “sizes” of the holes and compare them with corresponding ionic radii. The size of the interstitial site for an $A15$ structure

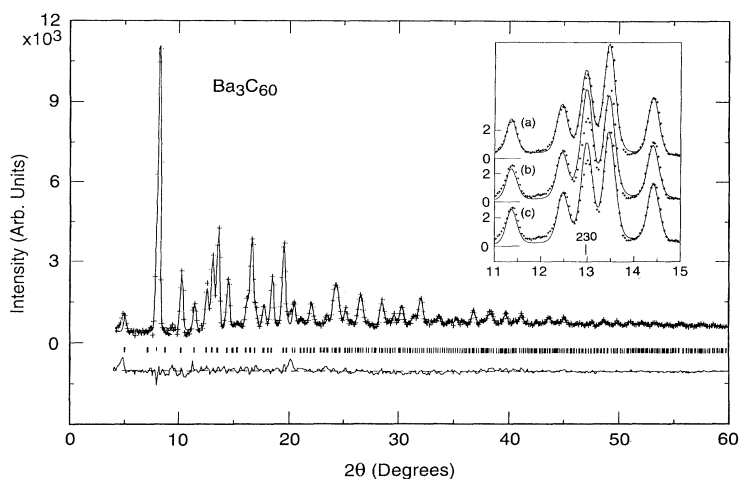


FIG. 2. Rietveld refinement fit (solid line) of the $Pm\bar{3}n$ $A15$ phase [model (a) of Fig. 1] provides the best description of the diffraction data (+). These fits to models of Fig. 1, shown in the inset, differ most substantially for the 230 intensity.

TABLE I. Structural parameters of Ba_3C_{60} . Space group: $Pm\bar{3}n$ (No. 223), $a_0 = 11.343(3)$ Å, $R_i = 11.9\%$, 411 reflections. $R_i = \sum |f_{\text{obs}} - f_{\text{calc}}| / \sum f_{\text{obs}}$.

Atom	Site	x	y	z	U_{iso} (Å ²)
C1	24k	0	0.3138(7)	0.0646(1)	0.033(7)
C2	48l	0.1292(3)	0.1046(2)	0.2738(6)	0.033(7)
C3	48l	0.0646(2)	0.2091(5)	0.2338(5)	0.033(7)
Ba	6c	0.2500	0	0.5	0.022(1)

Distances (Å)		
C1-C2	1.4658(35)	C2-Ba 3.142(6)
C1-Ba	2.981(7)	C3-Ba 3.385(5)

with a unit cell of $a = 11.343$ Å, is 1.32 Å, which is remarkably close to the 1.33 -Å radius of the doubly ionized barium atom. This suggests that divalent barium cations in $A15$ structure are close to their fully ionized state.

On the basis of this structural description, we now turn to the problem of energetics. First, how can the observed stability of the $A15$ structure over filled fcc for Ba be understood? It has been argued previously¹² that Madelung energy is the single most important contribution to the structural energy. For $\text{Ba}_3^{2+}\text{C}_{60}^{6-}$, computations using the same interball distance (10.21 Å) give a Madelung energy per C_{60} of -29.82 eV for the hypothetical fcc phase and -29.01 eV (0.81 eV higher) for the $A15$ phase. In fact, though this interball distance is probably appropriate for the fcc phase (Ba^{2+} and K^+ have the same ionic radius 1.33 Å), it is considerably larger than the interball distance 9.82 Å observed in $\text{Ba}_3^{2+}\text{C}_{60}^{6-}$, and this constant interball distance comparison overly favors the fcc phase. It seems that the lattice constants are set, not by a hard-core radius of C_{60} , but by the requirement that the tetrahedral hole be able to accommodate an ion the size of K^+ or Ba^{2+} . If we instead compare the Madelung energy per C_{60} for hypothetical fcc $\text{Ba}_3^{2+}\text{C}_{60}^{6-}$ (-29.82 eV) at the $\text{K}_3^+\text{C}_{60}^{3-}$ experimental lattice constant 14.253 Å with that of $A15$ $\text{Ba}_3^{2+}\text{C}_{60}^{6-}$ (-29.77 eV) at the experimental lattice constant 11.343 Å, we find that the relative Madelung energy of the $A15$ phase has been lowered from 0.81 to 0.05 eV per C_{60} . For the same size tetrahedral hole, the $A15$ phase has a lower interball distance, which results in the significantly lowered Madelung energy.

With such a small Madelung energy difference, other contributions to the structural energy are important in determining the lowest-energy structure. The observed preference of the Ba for the four-pentagon hole in the $A15$ structure suggests that the C_{60} cation interaction energy is lower for the molecular orientation with a pentagon facing the cation than for a hexagon facing the cation. This results from anisotropic distribution of the added charge over the C_{60} molecule,¹⁵ which could be interpreted in terms of electron deficiency in the five-membered rings of the molecules. This interaction would favor the $A15$ structure over the fcc structure, which has only hexagon holes. Further, molecular relaxations were found, by Andreoni, Gygi, and Parrinello,¹⁶ to contribute about 1 eV per C_{60} in bcc-packed K_6C_{60} and to be very much smaller in fcc-packed K_3C_{60} . For bcc-packed

$\text{Ba}_3^{2+}\text{C}_{60}^{6-}$, we expect an energy gain similar to that of K_6C_{60} , which has the same charge state and packing of the C_{60} molecules and a similar interball distance of 9.86 Å. This could be verified by similar first-principles calculations for $\text{Ba}_3^{2+}\text{C}_{60}^{6-}$ in the fcc and $A15$ structures. This extra 1 eV per C_{60} can account for the observed stability of the $A15$ phase.

Given these energetically favorable aspects of the $A15$ structure for $\text{Ba}_3^{2+}\text{C}_{60}^{6-}$, it is necessary to review the chemical trends observed with other cations. For example, the $x = 3$ fullerite with the much smaller cation Ca^{2+} (ionic radius 0.99 Å) is stable not in the $A15$ structure, but in the fcc structure. In this case, we suggest that the lattice constant needed to get a tetrahedral hole this small in the bcc packing results in an interball distance below the “hard-core” radius, which then sets a lower limit to the lattice constant and a reduced Madelung energy gain for the $A15$ structure.

The relative stability of K_3C_{60} in the fcc phase cannot be understood on the basis of the K^+ ionic radius, which is in fact equal to the Ba^{2+} ionic radius 1.33 Å, but must result from the difference in the charge state of the ball. It may be that the orientation dependence of C_{60} dopant interaction changes with the charge state, and that in the 3-state, the C_{60} cation energy is lower for the hexagon orientation, thus favoring the fcc structure with its perfectly oriented hexagon hole. Additionally, the “hard-core” radius of C_{60} could depend on the charge state and packing, putting the lower interball distance in the $A15$ K_3C_{60} phase below the hard-core radius for bcc-packed C_{60}^{3-} , though not for bcc-packed C_{60}^{6-} . If the lower interball distance in the bcc-packed C_{60}^{6-} is the result of molecular relaxation, then a reduction in the relaxation energy for hypothetical bcc-packed C_{60}^{3-} would result in a larger interball distance.

Using known ionic radii and observed lattice constants of known phases, we can summarize this discussion in a schematic plot of fcc and $A15$ energies (the latter including the molecular relaxation contribution) versus ionic radius, where at each value of the ionic radius the lattice constants of the two phases are the lower of the “hard-

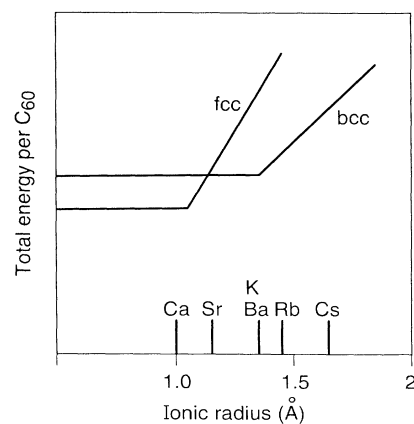


FIG. 3. Variation of the model fcc and bcc structural total energies with the cation radius.

core" distance for that packing and charge state and of that required to accommodate an ion of the given radius in the tetrahedral hole. Figure 3 shows a simple model of the total energy of the fcc and bcc (*A15* for 2+ ions and *Im $\bar{3}$* for 1+ ions) structures as a function of the *A* ionic radius. For very small cations, the lattice constant of both structures is set by the "hard-core" C₆₀ interball distance of about 9.8–9.9 Å and fcc is favored. The total energies of both structures increase with increasing lattice constant once the ionic radius exceeds the size of the tetrahedral hole, with the critical value for fcc being smaller than for bcc. The lattice constant of fcc Ca₃²⁺C₆₀⁶⁻ was used to determine the "hard-core" distance for fcc-packed C₆₀⁶⁻ to be 9.9 Å, virtually the same as for bcc-packed C₆₀⁶⁻. The ionic radius of Sr, 1.14 Å, falls midway between Ca and Ba, probably slightly beyond the change in slope of the fcc curve. In this range, fcc and *A15* are expected to be extremely close in energy and we cannot unambiguously predict within this simple picture which will be more stable.

In general, both experiment¹⁷ and theory¹⁸ suggest that in alkaline-earth-doped fullerites strong hybridization may take place between the dopant and the fullerite

bands. However, recent resistivity measurements¹⁹ performed on Ba_{*x*}C₆₀ thin films find a local maxima near *x* = 3. This observation is consistent with a simple rigid band model for Ba₃C₆₀, with a completely filled *t*_{1u}-derived band and a vanishing density of states at the Fermi level.

In conclusion, investigation of doped fullerite systems should continue to yield new compounds and crystal structures. As illustrated by the case of the *A15* structure Ba₃C₆₀, this may be accompanied by a further increase in the variety of types of molecular orientational order, which we suggest provides a useful characterization of the structure. Also, the structural energetics of new compounds can be predicted and explained by simple models such as that described in this paper, which can form the basis for more quantitative first-principles studies and for the identification of particular systems on which to focus effort in solving the challenging synthesis problems arising in doped fullerite systems.

We thank T. Siegrist, D. W. Murphy, M. A. Schluter, A. F. Hebard, J. C. Phillips, M. J. Rosseinsky, and J. Tully for valuable discussions.

-
- ¹A. F. Hebard, M. J. Rosseinsky, R. C. Haddon, D. W. Murphy, S. H. Glarum, T. T. M. Palstra, A. P. Ramirez, and A. R. Kortan, *Nature* **350**, 600 (1991).
- ²K. Holczer, O. Klein, S.-M. Huang, R. B. Kaner, K.-J. Fu, R. L. Whetten, and F. Diederich, *Science* **252**, 1154 (1991).
- ³M. J. Rosseinsky, A. P. Ramirez, S. H. Glarum, D. W. Murphy, R. C. Haddon, A. F. Hebard, T. T. M. Palstra, A. R. Kortan, S. M. Zahurak, and A. V. Makhija, *Phys. Rev. Lett.* **66**, 2830 (1991).
- ⁴C.-C. Chen, S. P. Kelty, and C. M. Lieber, *Science* **253**, 886 (1991).
- ⁵A. R. Kortan, N. Kopylov, S. Glarum, E. M. Gyorgy, A. P. Ramirez, R. M. Fleming, F. A. Thiel, and R. C. Haddon, *Nature* **355**, 529 (1992).
- ⁶A. R. Kortan, N. Kopylov, S. Glarum, E. M. Gyorgy, A. P. Ramirez, R. M. Fleming, O. Zhou, F. A. Thiel, P. L. Trevor, and R. C. Haddon, *Nature* **360**, 566 (1992).
- ⁷R. M. Fleming, M. J. Rosseinsky, A. P. Ramirez, D. W. Murphy, J. C. Tully, R. C. Haddon, T. Siegrist, R. Tycko, S. H. Glarum, P. Marsh, G. Dabbagh, S. M. Zahurak, A. V. Makhija, and C. Hampton, *Nature* **352**, 701 (1991).
- ⁸O. Zhou, J. E. Fischer, N. Coustel, S. Kycia, Q. Zhu, A. R. McGhie, W. J. Romanow, J. P. McCauley, A. B. Smith III, and D. E. Cox, *Nature* **351**, 462 (1991).
- ⁹For a recent review see *Fullerenes*, edited by G. S. Hammond and V. J. Kuck, ACS Symposium Series No. 481 (American Chemical Society, Washington, D.C., 1992).
- ¹⁰P. W. Stephens, L. Mihaly, P. L. Lee, R. L. Whetten, S.-M. Huang, R. Kaner, F. Deiderich, and K. Holczer, *Nature* **351**, 632 (1991).
- ¹¹D. W. Murphy, M. J. Rosseinsky, R. M. Fleming, R. Tycko, A. P. Ramirez, R. C. Haddon, T. Siegrist, G. Dabbagh, J. C. Tully, and R. E. Walstedt, *J. Phys. Chem. Solids* **53**, 1321 (1992).
- ¹²K. M. Rabe, J. C. Phillips, and J. M. Vandenberg (unpublished).
- ¹³S. Mendelson, *Phys. Status Solidi A* **98**, 133 (1986).
- ¹⁴W. C. Hamilton, *Acta. Crystallogr.* **18**, 502 (1965).
- ¹⁵S. C. Erwin and M. R. Pederson, *Phys. Rev. Lett.* **67**, 1610 (1991).
- ¹⁶W. Andreoni, F. Gygi, and M. Parrinello, *Phys. Rev. Lett.* **68**, 823 (1992).
- ¹⁷Y. Chen, D. M. Poirier, M. B. Jost, C. Gu, T. R. Ohno, J. L. Martins, J. H. Weaver, L. P. F. Chibante, and R. E. Smalley, *Phys. Rev. B* **46**, 7961 (1992).
- ¹⁸S. Saito and A. Oshiyama, *Solid State Commun.* **83**, 107 (1992).
- ¹⁹R. C. Haddon, G. P. Kochanski, A. F. Hebard, A. T. Fiory, R. C. Morris, and A. S. Perel (unpublished).

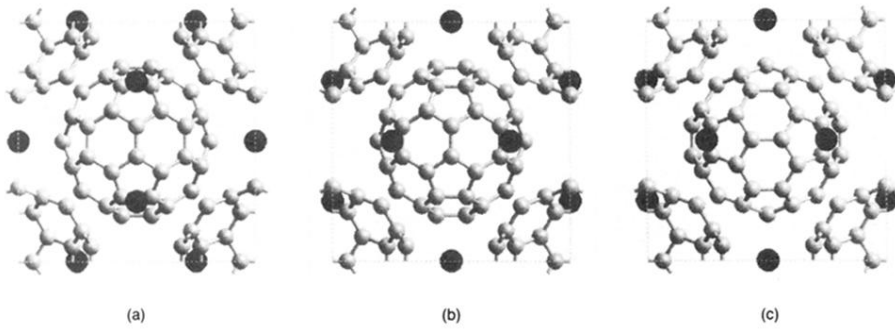


FIG. 1. Structural models of the Ba_3C_{60} A15 phase. Barium cations occupying the interstitial sites defined by five-membered rings (a), and six-membered rings (b) of the neighboring molecules. Orientationally aligned molecules define the $Pm\bar{3}$ structure in (c).